Experimental investigations on the cyclic behavior and fatigue of extruded 2017 aluminum alloy

Abdelghani May[1,2], Lakhdar Taleb[2,*], Mohamed el Amine Belouchrani[1]

[1]Laboratoire Génie des Matériaux, EMP, BP 17 Bordj El-Bahri Algiers, Algeria
[2]INSA/GPM, BP 08 avenue de l'université, 76801 St Etienne du Rouvray Cedex, France
* Corresponding author: lakhdar.taleb@insa-rouen.fr

Abstract The present work is devoted to the study of the anisotropic behavior of an extruded aluminum alloy under cyclic loading in axial and shear directions at room temperature. First, we have studied the elastoplastic behavior through the evolution of the isotropic and kinematic hardening evaluated considering the stress-strain loops in axial and shear directions. Second, we have investigated the fatigue damage of the material in both directions. The observed lifetimes seem rather short regarding the elastic shakedown obtained at the steady state.

Keywords: Anisotropic behavior, Extruded alloys, isotropic and kinematic hardening, cyclic plasticity.

1. Introduction

Aluminum alloys are frequently selected for many applications where low density and high strength-to-weight ratios are required. Thus, 2XXX series are currently being used as the main structure in components which are often subjected to cyclic loading. Therefore, we devote this work to the investigation of mechanical anisotropy in the cyclic behavior of aluminum alloy through stress controlled tests.

Many authors focused their work on the influence of microstructural and metallurgical states on the behavior of age hardened aluminum alloys during cyclic loading [1-6]. Furthermore, the anisotropy of mechanical behavior in metallic alloys during monotonic deformation was investigated by several authors [7-9]. Firstly, this anisotropy was discussed only for rolled or extruded alloys, such as metal sheets. Achani et al. [10] characterized the plastic anisotropy of extruded aluminum alloys 7003 and 6063 by uniaxial tensile testing and disc compression tests, showing that the increase of flow stress is directional and most significant for orthogonal sequences. On the other hand, some authors [11, 12] observed a strong anisotropic flow behavior between the rolling and transverse direction of rolled aluminum alloys during uniaxial tests. Recently, other authors have studied the effect of plastic anisotropy on the mechanical behavior of a rolled aluminum alloy 7075 [13]. They stated that the crystallographic texture and grain morphology gave rise to a strong plastic anisotropy in the rolled aluminum plate; they observed that the effect of plastic anisotropy is less for notched than for smooth tensile tests. Recently, Saï et al. [14] have focused their work on modeling the cyclic behavior of aluminum alloys. They up-dated the multi-mechanism models to be applied to anisotropic materials such as 2017 aluminum alloy.

The fatigue behavior of aluminum alloys under stress control tests has also been investigated for many years [3, 15, 16]. It has been shown that a microstructure strengthened by nonshearable and hard particles is usually preferable to resist more at fatigue crack initiation [17]. Similarly, Malekjani et al. [18] demonstrated the beneficial effect of precipitates at the core of the sample on the fatigue life during cyclic loading. Furthermore, according to [19, 20], fatigue evolution is not accompanied by any apparent modification of either the form or the aspect of the test specimen. Flaceliere et al. [21] studied the effect of shakedown phase on cyclic behavior of polycrystalline materials. They stated that the hardening saturation effect at the beginning of the fatigue lifetime and damage-induced softening at the end of fatigue lifetime describe all the cyclic behavior during loading. Despite all these studies, aluminum alloy anisotropy and its influence on the evolution of the cyclic behavior is not yet well investigated. Therefore, we devote the present paper to the following investigations performed on a 2017 aluminum alloy at room temperature:

- Study of the mechanical anisotropy in cyclic behavior through the stress-strain responses.
- Investigation of the cyclic hardening using the concept of isotropic and kinematic hardenings and their dependence on the loading direction.
- Correlation between the rate of isotropic hardening, elastic shakedown and fatigue lifetime.

This article is composed of three parts. The first section is devoted to the description of our experimental procedure, while the second section presents the results obtained about the cyclic behavior and their discussions. In the last section, the results obtained concerning fatigue damage evolution will be discussed.

1. Experimental procedure

1.1 Material

All the investigations carried out in this study were performed at room temperature using a 2017 aluminum alloy. The chemical composition is given in Table 1.

Table 1. Chemical composition of the material used (wt %)

Cu	Mg	Mn	Fe	Si	Zn	Ni	Cr	Al
3.9 – 4.0	1.1 – 1.2	0.7 – 0.8	0.5 – 0.6	0.6 – 0.7	< 0.21	< 0.16	< 0.10	Bal.

It is well-known that the hardening of this alloy arises from Al_2Cu and Al_2CuMg precipitation, provided that particles are finely and densely distributed. However, these precipitations lead to heterogeneity phenomena of the material that can generate anisotropy in mechanical behavior.

1.2. Specimens and experimental device

All the specimens were machined from solid bars extruded in the axial direction and a tubular shaped sample with two massive heads is used; its gage length is 46 mm in the central part where an extensometer of 25 mm gage length is installed. In this zone, the outer and inner diameters are 20 mm and 17 mm, respectively (Fig. 1), making it possible to have relatively thin tubes.

To ensure the same microstructural state of the material all specimens were heat treated according to a T3 thermal cycle (Fig. 2). The tests were performed with a MTS axial-torsional servo-hydraulic machine, an extensometer was used to measure the axial and torsional displacements in the central area of the specimen. The gage length of the extensometer is 25 mm for the shearing tests and 12 mm in tension/compression tests.

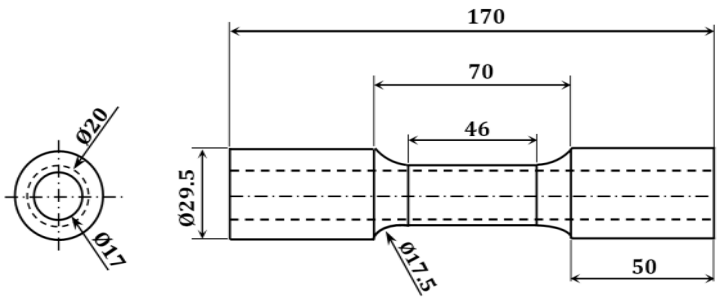

Figure 1. Geometry of the specimen used in the study

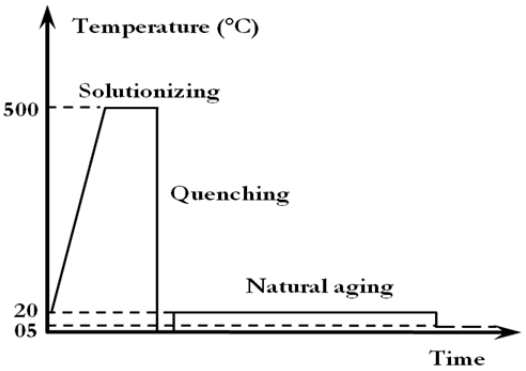

Figure 2. Sequences of the heat treatment applied to specimens

A permanent cooling of the specimen is applied during tests in order to remain close to room temperature and minimize the effect of heating due to the dissipation process observed under cyclic loading in the plastic domain.

1.3. Tests performed

Two types of stress-controlled tests were performed in this study. First, a cyclic tension-compression loading is applied with a zero mean stress (R = -1). In order to ensure a ‘‘perfect” uniaxial stress state, all the tests were performed under bi-axial controlled conditions, where the torque is set at zero (Fig. 3a). The second type is a cyclic shear tests applied with zero axial stress on six identical specimens (Fig. 3b). The applied frequency for both tests is 0.5 Hz during the first 400 cycles and 1 Hz after.

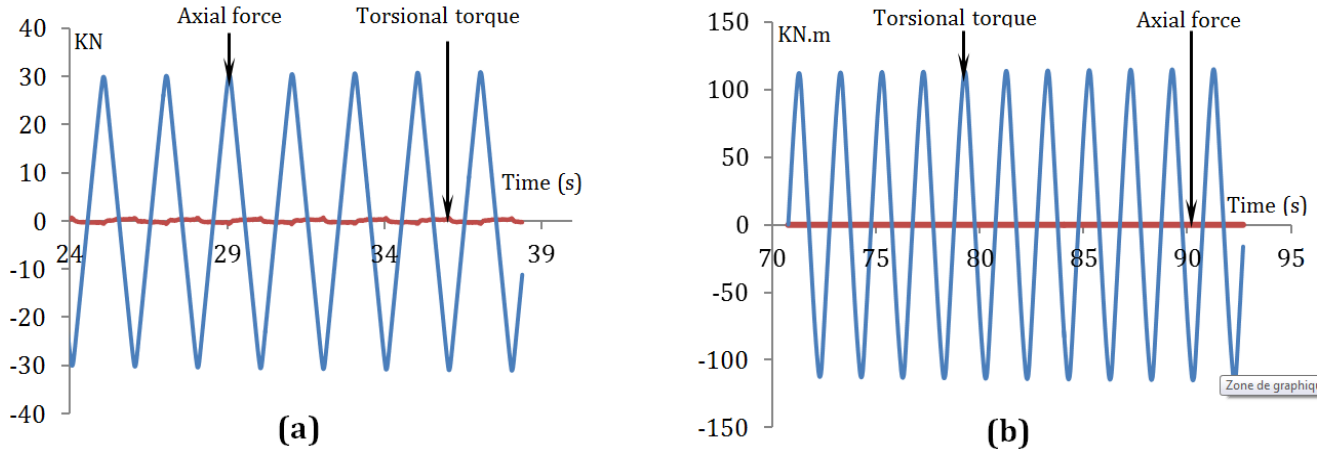

Figure 3. The two types of stress controlled tests performed in the study. (a) Cyclic tension-compression under zero shear stress; (b) Cyclic shearing stress under zero axial stress

The list of the tests performed in this study is shown in Table 2 where**:**

- σ_{zz} : is the maximum stress applied in tension – compression.
- $\sigma_{\theta z}$: is the maximum stress applied in shearing.
- σ^{eq} : is the equivalent maximum shearing stress using Von Mises criterion.

Note that the equivalent shearing amplitudes were calculated using Von Mises criterion.

Table 2. List of the tests performed in this study

Tension-compression tests		Shearing tests			
σ_{zz} (MPa)	Reference	Torque (N.m)	$\sigma_{\theta z}$ (MPa)	σ^{eq} (MPa)	Reference
240	ax240	80	98	170	sh80
260	ax260	90	110	190	sh90
280	ax280	100	122	211	sh100
300	ax300	110	136	235	sh110
320	ax320	120	148	256	sh120
340	ax340	130	160	277	sh130
360	ax360				

2. Results of the cyclic behavior

Before the analysis of the cyclic behavior, let us first see the evolution of lifetimes obtained under the axial and shear directions in Fig. 4.

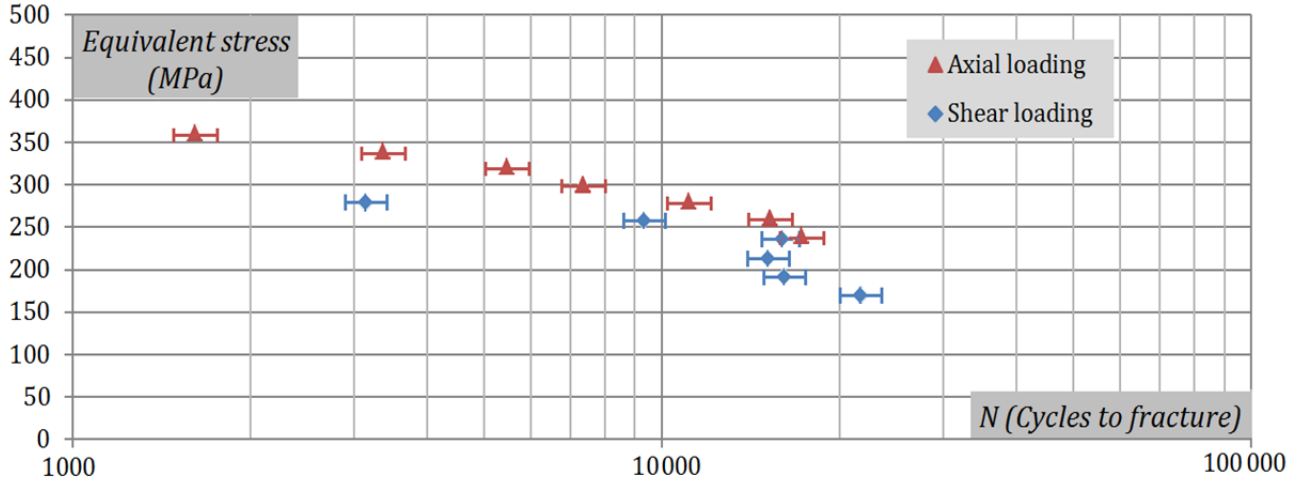

Figure 4. Wohler curve of a 2017 aluminum alloy for the axial and the shear loadings.

Note that each point of these curves represents the average result of at least two tests. Indeed, we have a more or less linear increase in the number of cycles to failure, when the applied maximum stress decreases. According to the two curves presented in Fig. 4, we can also remark anisotropy between the two directions in fatigue life. In fact, we notice a significant difference between lifetimes in axial and shear directions. Indeed, for the same equivalent stress amplitude, lifetime in the axial direction is higher compared to that in the shear direction. However, one can expect the opposite observation in case of strain control.

2.1. Test results under axial loading

To better represent the evolution of the stress-strain loops, we plot for each test and in the same graph the first and the stabilized loops. The first loop is taken when the maximum set-point stress is reached. The stabilized stress-strain loop is chosen at mid-life where the strain hardening does not evolve significantly. In Fig 5, we depict six graphs representing axial tests.

2.2. Test results under shear loading

In Fig. 6a, we depicted the equivalent stress versus the equivalent strain, where the maximum stress in Von Mises equivalence is 277 MPa. In this case, we have the plastic flow which remains high even in mid-life. However, in Fig. 5a, the maximum axial stress is 360 MPa, the plastic flow decreases gradually until it stops before mid-life and the behavior becomes almost elastic. This behavior suggests the anisotropy of the material between the axial and shear directions.
Such anisotropy appears also in the yield stress given in Table 3 where the axial elastic limit is 207 MPa while the equivalent shearing one is only 142 MPa. This behavior will be discussed in more details in the next section.

Table 3 Mechanical properties of the 2017 aluminum alloy determined from monotonic loading

Axial yield stress at 0.01%	Axial yield stress at 0.2%	Young's modulus E	Equivalent shear yield stress at 0.01%	Coulomb's modulus G
207 MPa	284 MPa	72 GPa	142 MPa	23.5 GPa

2.3. Discussion

To study the cyclic behavior of 2017 aluminum alloy in plasticity, we have to investigate the evolution of the elastic domain in the stress space which is usually represented by a translation of its center (kinematic hardening) and the expansion (isotropic hardening) of its size. In the case of isotropic material, the yield surface expands generally in a homogeneous manner all over the

directions. However, this behavior remains debatable for the majority of aluminum alloys under a high stress loading.
As it is not an easy task to identify the linear part of the stress–strain diagram and therefore the elastic domain, we have admitted a small equivalent plastic strain offset equal to 0.0001. The isotropic and kinematic hardening variables were evaluated in each cycle using the same formulation used in [22]**.** In Fig. 7, we show how the isotropic and kinematic cyclic hardening variables are estimated according to:

$$\begin{cases} |\sigma_{max} - X| - R - \sigma_y = 0 \\ |\sigma_{off} - X| - R - \sigma_y = 0 \end{cases} \text{ And since } \begin{cases} \sigma_{max} - X > 0 \\ \sigma_{off} - X < 0 \end{cases} \qquad \text{Then, } \begin{cases} R = \frac{\sigma_{max} - \sigma_{off}}{2} - \sigma_y \\ X = \frac{\sigma_{max} + \sigma_{off}}{2} \end{cases}$$

R and X represent a first approximation of the isotropic and kinematic hardening variables respectively; σ_{max} is the maximum equivalent stress reached in the considered cycle while σ_y is the initial elastic limit deduced from the first cycle. σ_{off} is the stress corresponding to 0.0001 of plastic strain offset obtained during the unloading (see Fig. 7a). In Fig. 7b, we depicted two experimental examples. The obtained results are given in Fig. 8 and Fig.9.
According to the results obtained under axial loadings, we note that the increase of R is slightly high during the first cycles, where the maximum stress set-point is reached (Fig. 8a); this progression seems to be less important after the 40 first cycles, which depends strongly on the maximum stress of each test. However, the X variable decreases in all the tests (Fig. 8b), especially when the maximal applied stress is slightly high.

The same work was done for shear loading; the obtained results are plotted in Fig. 9 which shows that shear loading leads to more kinematic hardening than the isotropic one when the maximum applied shear stress is relatively small. But when the shear stress is relatively high, we obtained a significant hardening for both isotropic and kinematic types.
Comparing the two types of the tests, we deduce once again a relatively significant anisotropy in cyclic behavior. In fact, the isotropic hardening increases cyclically in the two directions of the tests but more significantly in the axial one. Furthermore, kinematic hardening decreases in both directions but more significantly in the axial one.

The amount of anisotropy obtained in the two directions of loading can be attributed to the nature and the size of dispersed precipitates in the alloy. This anisotropy is even larger when the maximum stress is high, because of the increase in the resistance of the precipitates to the dislocation movements which become more and more dense.

Furthermore, we can notice that the evolution of isotropic hardening may be correlated with the evolution of the shakedown limit. In order to understand this relationship, we have to investigate the behavior of our material in shakedown phenomenon where the mechanical behavior becomes purely elastic. The plastic strain is used to estimate the shakedown occurrence. We assume that:
$\varepsilon = \varepsilon^e + \varepsilon^p$ where ε^e and ε^p are respectively the elastic and the plastic strains.
With this assumption, we estimate the plastic deformation at any point of the stress-strain loops. Then, we assume that shakedown state is reached when the plastic strain of a given cycle is less than 0.0001. This is a reasonable assumption, since beyond this limit, it becomes very difficult to assess both isotropic and kinematic hardening (R and X). The procedures presented in **Error! Reference source not found.** illustrate the method used to determine the occurrence of the shakedown phenomenon from the stress-strain loops and from the ε^p versus number of cycle curves. However, when the maximum stress is too high, the behavior may be different. Indeed, the plastic strain reaches a periodic stabilized limit state; this phenomenon is referred as plastic

shakedown.

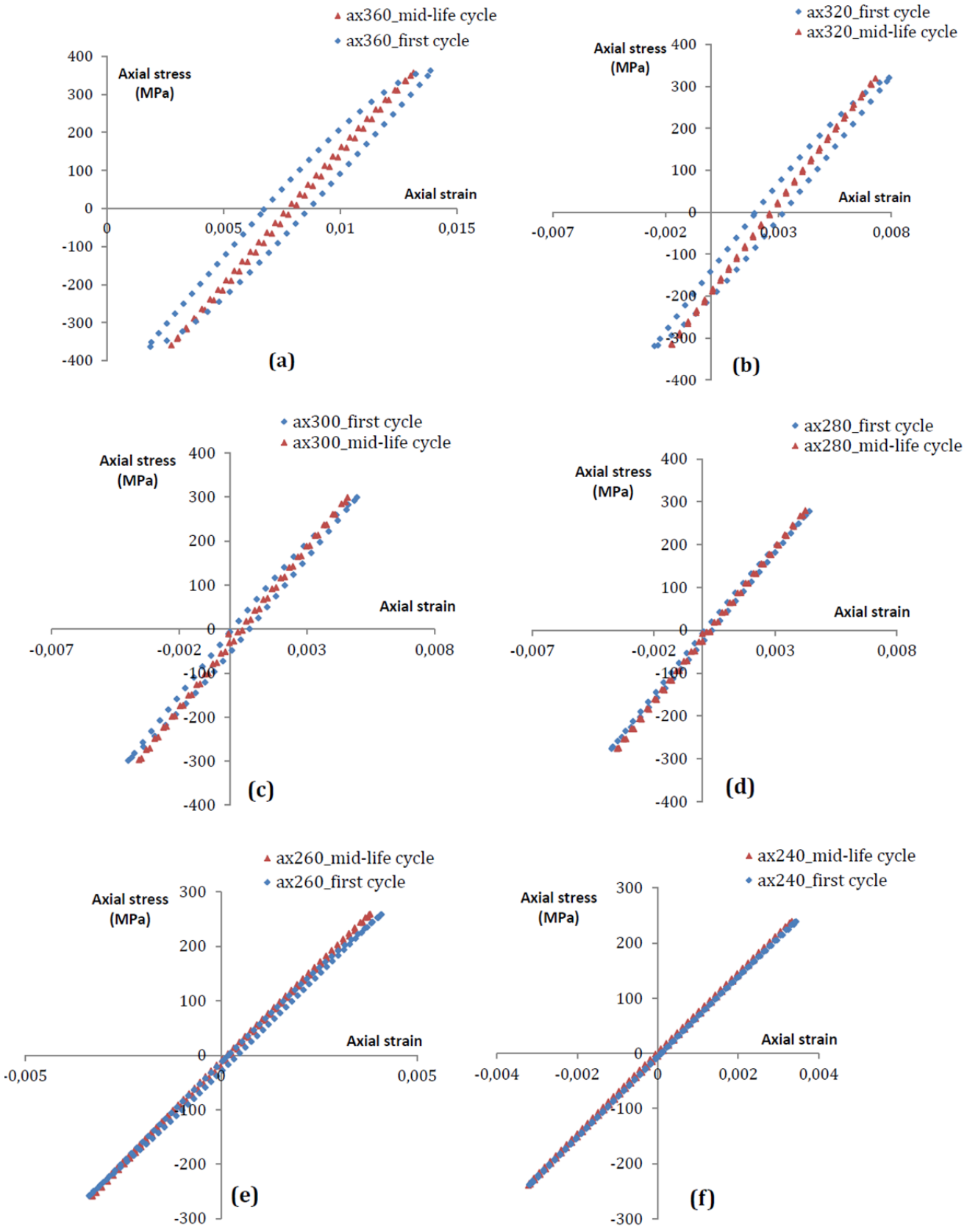

Figure 5. Axial stress–strain loops (first and mid-life cycles)

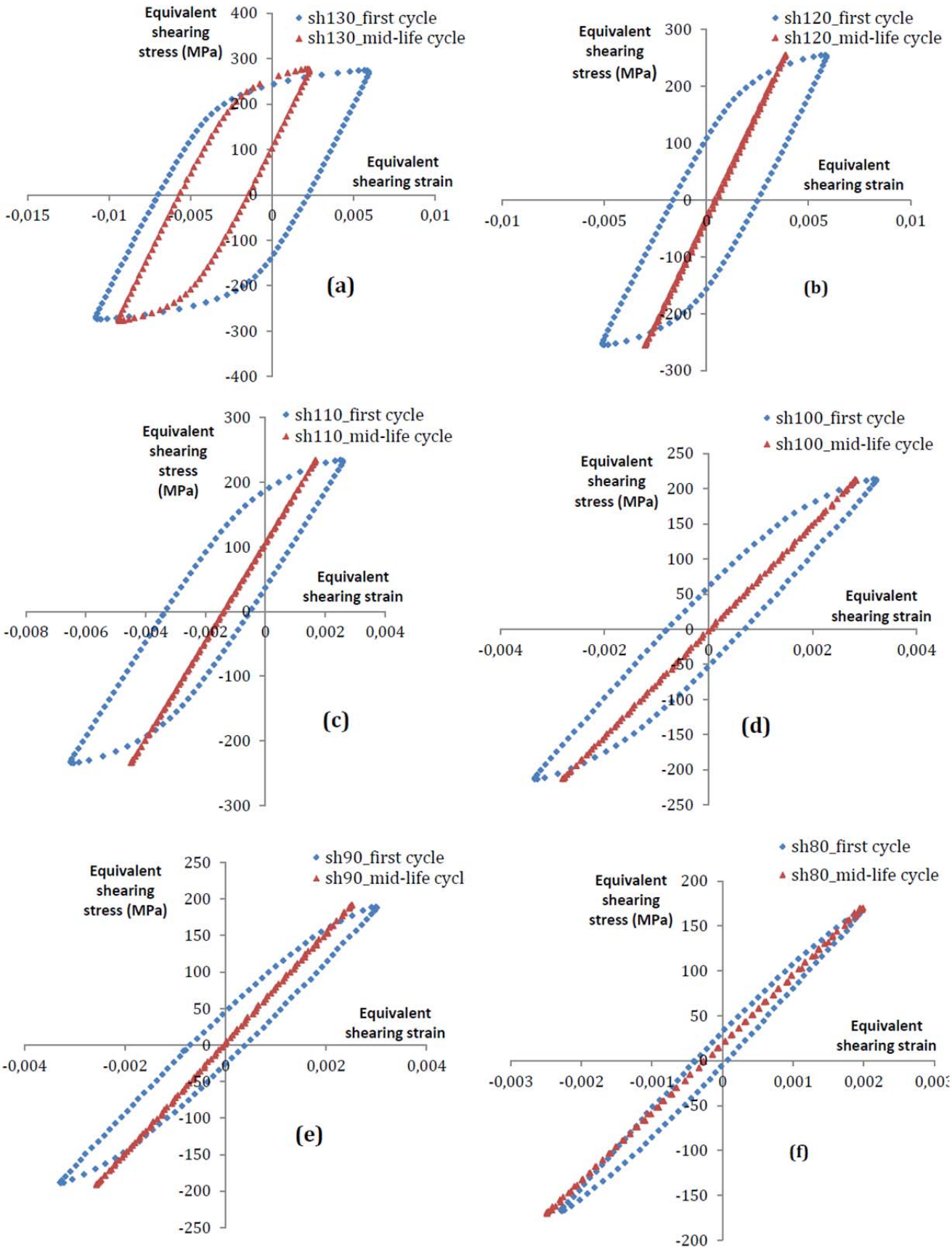

Figure 6. Results of the shear tests: Equivalent shearing stress ($\sqrt{3}\sigma_{\theta z}$) versus equivalent shearing strain ($2\varepsilon_{\theta z}/\sqrt{3}$) loops

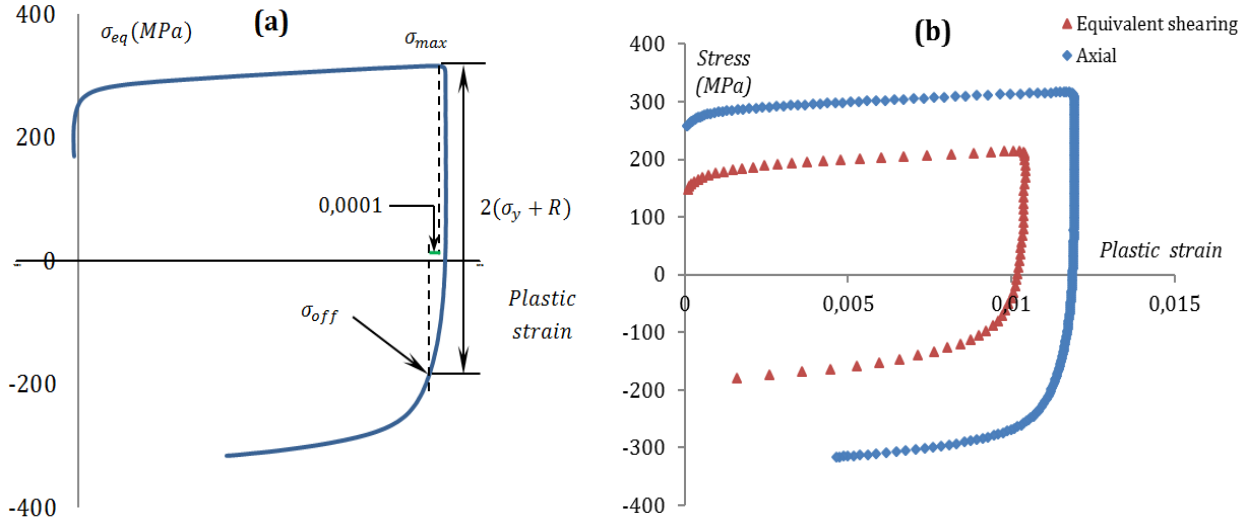

Figure 7. Evaluation of isotropic and kinematic hardenings: (a) Method of determining σ_{off} and σ_{max} (b) Experimental examples responses of the two test types performed in the present work

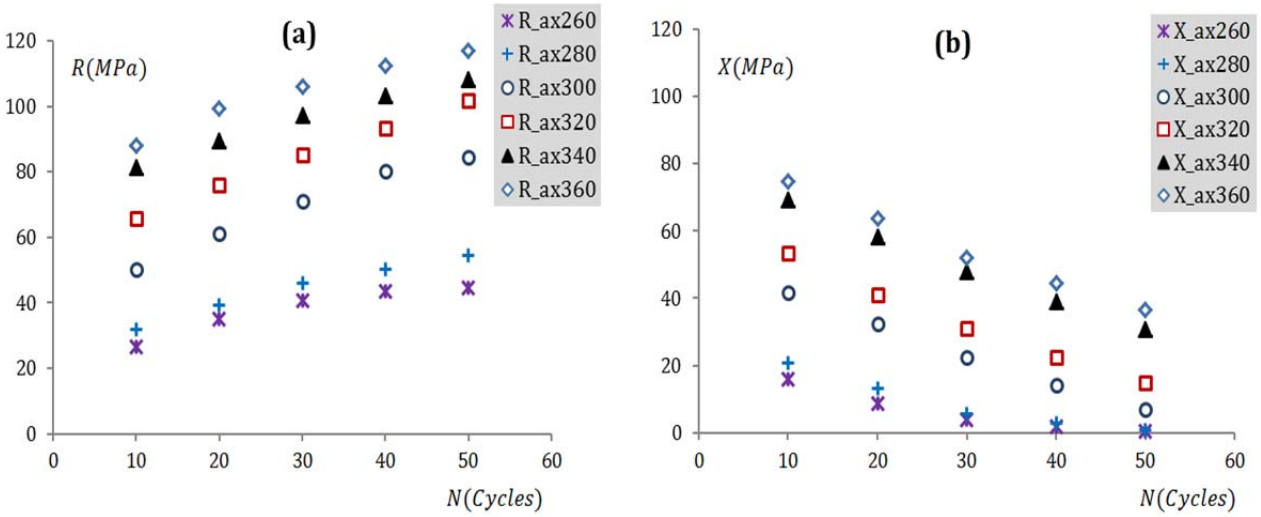

Figure 8. Evolution of cyclic hardening in axial loadings: (a) evolution of the variable R (pseudo isotropic hardening); (b) evolution of the variable X (pseudo kinematic hardening)

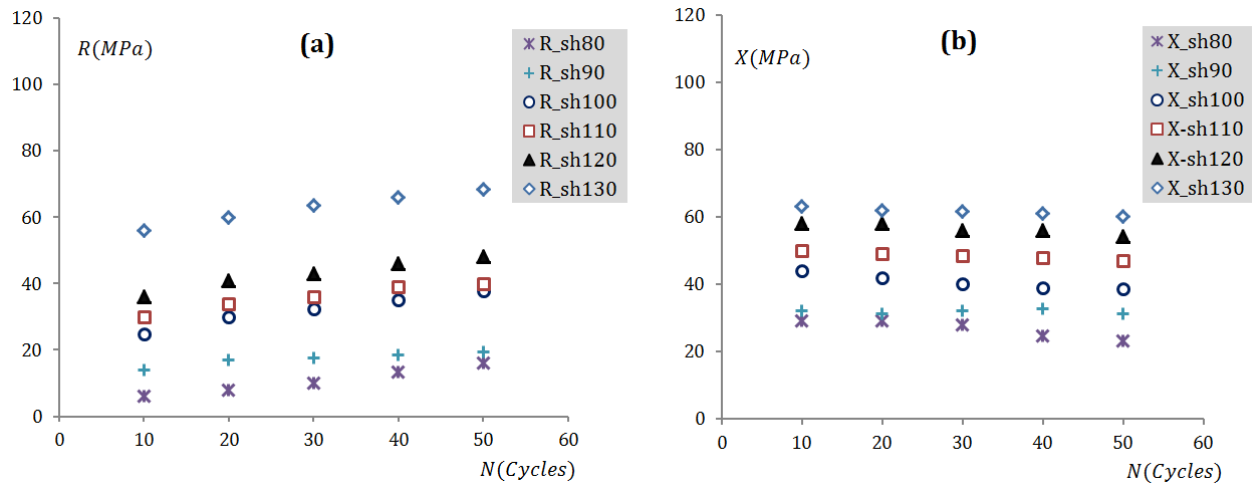

Figure 9. Evolution of cyclic hardening in shear loadings: (a) evolution of the variable R; (b) evolution of the variable X

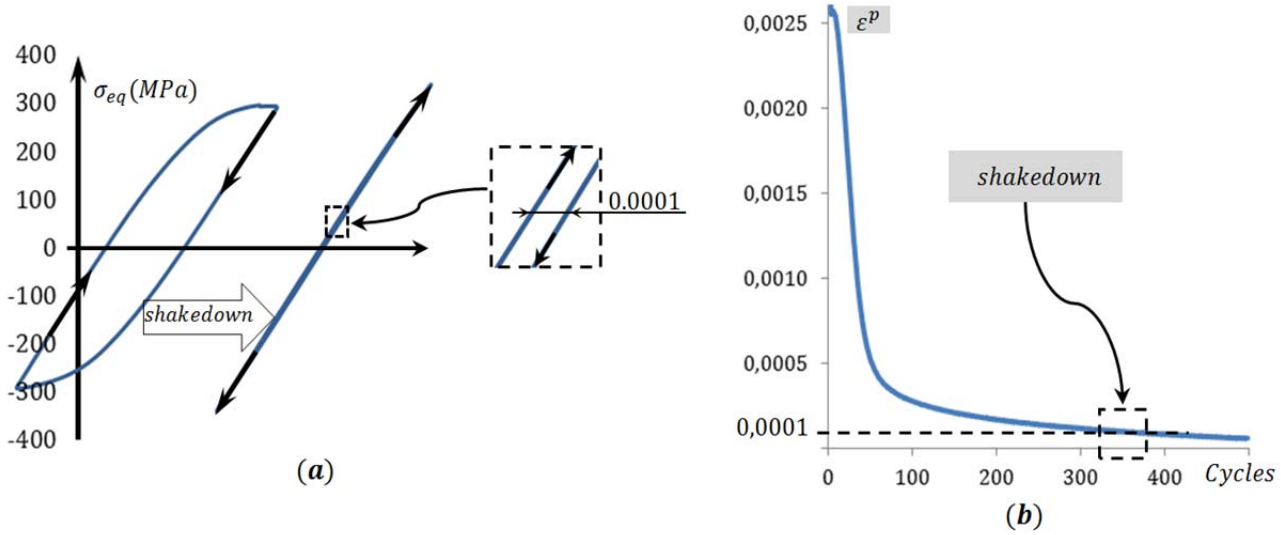

Figure 10. Evaluation of shakedown limit: (a) from the stress-strain loops; (b) from the plastic strain evolution

Following the previous method described in Fig. 10, we can easily evaluate the number of cycles corresponding to the elastic shakedown and the obtained results are given in Table 4. According to these findings and the results presented in Fig. 8 we deduce that a large increase of isotropic hardening leads to an early elastic shakedown despite the application of a high maximum stress. In other words, we can assert that a high isotropic hardening rate, found in the axial loadings, accelerates the shakedown limits.

Table 4. Evaluation of the number of cycles before the shakedown state

Test	ax240	ax260	ax280	ax300	ax320	ax340	ax360
Cycles to Shakedown	1st cycle	95th	77th	170th	320th	430th	>1400th

Under shear loading, elastic shakedown was also observed in the majority of the performed tests except in that of sh130, where the steady state is a closed elastic-plastic loop, but with very small accumulation of plastic deformation until final fracture. The obtained results for the shear loadings are summarized in Table 5.

Table 5. Evolution of the shakedown limit for the shearing tests

Test	sh80	sh90	sh100	sh110	sh120	sh130
Shakedown limit (Cycle)	180th cycle	390th	430th	800th	1600th	Plastic shakedown

According to these shakedown findings and the results presented in Fig. 9, we deduce the relationship between hardening and elastic shakedown in shear loading. Indeed, in these tests, the hardening rate (both isotropic and kinematic) is relatively low, leading to a very late shakedown.
The results presented in Table 5, confirm once again the anisotropic behavior of our alloy. Therefore, we deduce that elastic shakedown is quickly reached under axial loading but later in the shear one.
These results show that when the maximal stress is too high, the shakedown behavior is obtained after having a long time in plastic loading, which contributes largely to microstructural evolution of the specimen. Thus, the specimen breaks despite the elastic shakedown state is reached!

CONCLUDING REMARKS:

In the present work, the anisotropic behavior of a 2017 aluminum alloy is investigated through a stress controlled cyclic loading where two types of tests were performed. In the first one, seven tests using cyclic axial loading were done and in the second we have carried out six tests applying cyclic shear loading. The study is focused on the cyclic behavior as well as on the fatigue life: stress-strain loops, isotropic and kinematic hardenings and cyclic steady state were discussed.

The anisotropic behavior of our alloy is firstly deduced from the difference between the equivalent stress-strain loops obtained in the axial and shearing directions. The study of the cyclic behavior shows that isotropic hardening increases both in axial and shear directions, but more significantly in the axial one. On the other hand; isotropic hardening depends largely on the maximum amplitude of the loading for the two directions. Indeed, large stress amplitude generates a large amount of isotropic hardening which tends to grow during cyclic loading. The kinematic hardening decreases cyclically in both directions of loading, but more significantly in the axial tests where it tends to disappear very quickly. Furthermore, we can notice that the evolution of the isotropic hardening rate may be correlated with the evolution of the shakedown limit, where we can assert that a large isotropic hardening rate, found in the axial loadings, accelerates the shakedown limits. The same results obtained about shakedown limits allow us to conclude that the increase in maximum stress amplitude leads to a late elastic shakedown in the two directions of loading. Indeed, all the cycles done before elastic steady state, contribute largely to the nucleation of micro-voids causing microstructural evolution of the specimen and continue to grow despite the shakedown steady state. The anisotropy is also observed between the two directions in fatigue life as for the same equivalent stress amplitude, lifetime in the axial direction is higher compared to that in the shear direction. However, one can expect the opposite observation in case of strain control.

References

[1] J.B. Clark, Acta. Metall. 12 (1964) 1197-1201.
[2] C.T. Hahn, R. Simon, Eng. Fract. Mech. 5 (1973) 523-540.
[3] T.S. Srivatsan, E.J. Coyne Jr, Int. J. Fatigue. 8 (1986) 201-208.
[4] S.P. Ringer, K. Hono, Mater. Charact. 44 (2000) 101-131.
[5] R. Sadeler, Y. Totik, M. Gavgalı, I. Kaymaz, Mater. Des. 25 (2004) 439-445.
[6] T. Ludian, L. Wagner, Mater. Sci. Eng. A. 468–470 (2007) 210-213.
[7] R. Hill, J. Mech. Phys. Solids. 1 (1953) 271-276.
[8] F. Barlat, K. Lian, Int. J. Plast. 5 (1989) 51-66.
[9] H. Takahashi, H. Motohashi, S. Tsuchida, Int. J. Plast. 12 (1996) 935-949.
[10] D. Achani, O.S. Hopperstad, O.G. Lademo, J. Mater. Process. Technol. 209 (2009) 4750-4764.
[11] A.B. Lopes, F. Barlat, J.J. Gracio, J.F. Ferreira Duarte, E.F. Rauch, Int. J. Plast. 19 (2003) 1-22.
[12] N. Tardif, S. Kyriakides, Int. J. Solids. Struct. (2012) 00.
[13] M. Fourmeau, T. Børvik, A. Benallal, O.G. Lademo, O.S. Hopperstad, Int. J. Plast. 27 (2011) 2005-2025.
[14] K. Saï, L. Taleb, G. Cailletaud, Comput. Mater. Sci. 65 (2012) 48-57.
[15] T.B. Kermanidis, S.P. Pantelakis, D.G. Pavlou, Theor. Appl. Fract. Mech. 14 (1990) 43-47.
[16] Y. Murakami, K.J. Miller, Int. J. Fatigue. 27 (2005) 991-1005.
[17] E.A. Starke Jr, J.T. Staley, Prog. Aerosp. Sci. 32 (1996) 131-172.
[18] S. Malekjani, P.D. Hodgson, P. Cizek, I. Sabirov, T.B. Hilditch, Int. J. Fatigue. 33 (2011) 700-709.
[19] S.G. Pantelakis, P.V. Petroyiannis, K.D. Bouzakis, I. Mirisidis, Theor. Appl. Fract. Mech. 48 (2007) 68-81.
[20] A. May, M.A. Belouchrani, A. Manaa, Y. Bouteghrine, Proced. Eng. 10 (2011) 798-806.
[21] L. Flaceliere, F. Morel, A. Dragon, Int. J. Fatigue. 29 (2007) 2281-2297.
[22] L. Taleb, A. Hauet, Int. J. Plast. 25 (2009) 1359-1385.